Ichimura *et al. Earth, Planets and Space (2018) 70:125*
https://doi.org/10.1186/s40623-018-0895-4

Earth, Planets and Space

FULL PAPER

Open Access

Temporal variation in source location of continuous tremors before ash–gas emissions in January 2014 at Aso volcano, Japan

Misa Ichimura[1,2], Akihiko Yokoo[3*], Tsuneomi Kagiyama[3], Shin Yoshikawa[3] and Hiroyuki Inoue[3]

Abstract

Volcanic tremor is often observed to be associated with an increase in volcanic activity and during periods approaching eruptions. It is therefore of crucial importance to study this phenomenon. The opening of a new vent and subsequent ash–gas emissions was observed in the active crater (Nakadake crater) of Aso volcano, Japan, in January 2014. These events were considered to be associated with phreatomagmatic activity similar to the small events of 2003–2005. During the period from December 2013 to January 2014, a significant variation in the amplitude of continuous seismic tremors was observed corresponding to surficial volcanic activity. We estimated the tremor source locations for this two-month period by a three-dimensional grid search using the tremor amplitude ratio of 5–10 Hz band-pass filtered waveforms. The estimated source locations were distributed in a roughly cylindrical region (100–150 m in diameter) ranging from the ground surface to a depth of 400 m. Migration of the estimated source location was also identified and was associated with changes in volcanic activity. We assumed that the source locations coincided with a conduit system of the volcano, consisting of networks of fractures. This area is likely situated above the crack-like conduit proposed in previous studies. Before the 2014 event, an increase in gas-dominated volcanic fluid first caused an enlargement of the conduit zone, followed by the migration of further magmatic fluid through other pathways, which resulted in a subsequent ash–gas emission. Although we do not have sufficient information to discuss the causal relationship between these processes, it seems reasonable that continuous tremors might change the conduit conditions.

Keywords: Aso volcano, Volcanic continuous tremors, Source location, Pathway of volcanic fluids

Introduction

Volcanic tremors, which usually have frequencies from 1 to 9 Hz (McNutt 1992), are a sustained seismic oscillating signal, the duration of which ranges from minutes to days, months, or even longer in some cases. This phenomenon is often observed to be associated with an increase in volcanic activity and during periods approaching eruptions (e.g., Thompson et al. 2002; Almendros et al. 2007). It is therefore of crucial importance to monitor volcanic tremors in order to forecast future eruptions, although the exact physical mechanisms causing such tremors remain unclear and continue to be a subject of considerable debate. Tracking of the source location of volcanic tremors is one of the most critical and vital pieces of information with regard to volcanic hazard assessment.

Volcanic tremors have an emergent onset and an indiscernible phase arrival during oscillations. These characteristics make it impossible to correctly determine the source location of the tremor using the conventional approach to hypocenter determination. In order to overcome this drawback, Battaglia and Aki (2003) proposed a novel technique based on the spatial distribution of tremor amplitudes in a network consisting of a limited number of stations. This is often referred to as the amplitude source location (ASL) method (Kumagai et al. 2010). A fundamental assumption of the ASL method is that seismic waves associated with tremors observed

*Correspondence: yokoo.akihiko.5a@kyoto-u.ac.jp
[3] Aso Volcanological Laboratory, Institute for Geothermal Sciences, Kyoto University, 3028 Sakanashi, Aso, Kumamoto 869-2611, Japan
Full list of author information is available at the end of the article

at stations are a result of multiple scattering due to heterogeneity during seismic wave propagation. The validity of this assumption has been confirmed for the high-frequency band, i.e., > 5 Hz (Kumagai et al. 2010; Morioka et al. 2017). To date, a number of studies have applied the ASL method to volcanic tremors at, for example, Piton de la Fournaise volcano (Battaglia and Aki 2003), Etna volcano (Patanè et al. 2008), Cotopaxi and Tungurahua volcanoes (Kumagai et al. 2010), and Meakan-dake volcano (Ogiso and Yomogida 2012).

At the Nakadake crater of Aso volcano in the southwest of Japan (Fig. 1), notable magmatic eruptions, including frequent Strombolian explosions and voluminous ash venting, started in November 2014 and lasted until May 2015 (Yokoo and Miyabuchi 2015). Approximately one year in advance of these eruptions, in a two-month period from December 2013 to January 2014, we observed the opening of a new vent inside the crater and several ash–gas emissions, both of which occurred with significant changes in tremor amplitude (Figs. 2 and 3). We regarded these phenomena as the first and precursory anomalies for the latest magmatic eruptions. In the present study, in order to investigate this precursory activity, we estimated the source location of the observed volcanic tremors by applying an approach similar to the ASL method (Taisne et al. 2011). We hypothesized that continuous tremors (CTs) have a close relation to fluid transport processes in the shallow conduit system at Aso volcano. Based on our results for the spatiotemporal variation of the tremor source locations, we inferred the distribution of volcanic

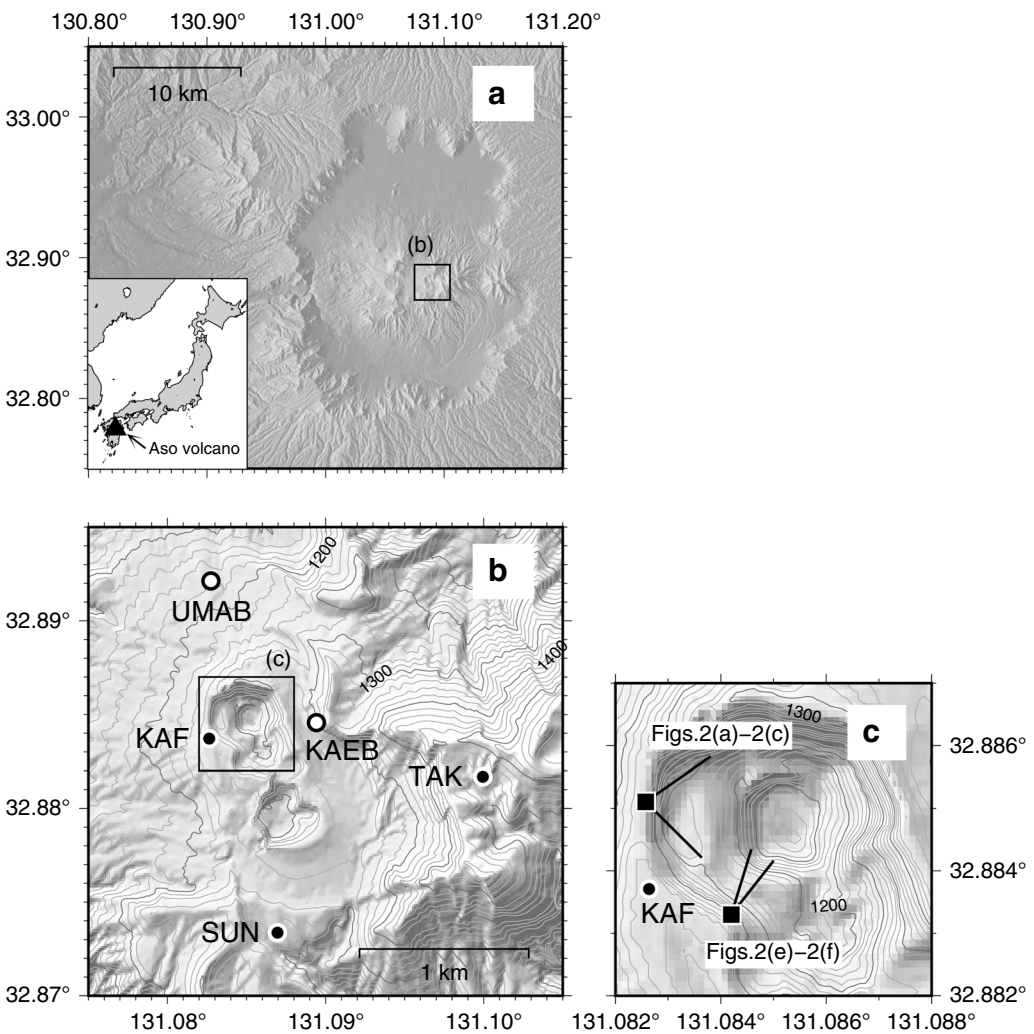

Fig. 1 Observation sites at Aso volcano, Japan. **a** Map of Aso volcano (Aso caldera) in Japan. **b** Five seismic stations around the active Nakadake crater of Aso volcano. Solid and open circles represent short-period and broadband seismometers, respectively. **c** Enlarged view around the active crater. The two black squares with fields-of-view indicate locations at which the photographs in Fig. 2 were taken

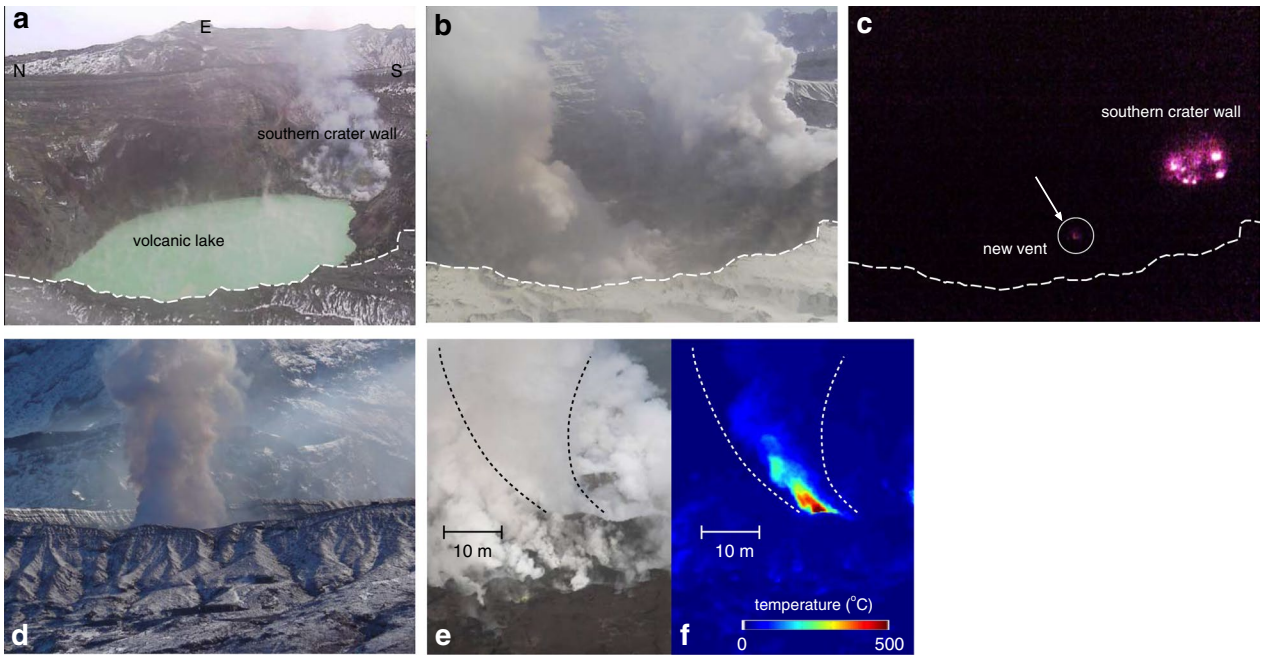

Fig. 2 Snapshots of the active crater from the west and southwest rim. **a** A volcanic lake was observed inside the Nakadake crater on 20 January 2013. A fumarolic region behind the lake (right-hand side of the image) was located on the southern crater wall. The orientation of the image is indicated by N, E, and S (see Fig. 1c). **b** On 25 December 2013, water was no longer present in the crater. **c** A new vent (indicated by the white circle) glows at the crater floor, similar to the southern crater wall (2 January 2014). Note that brightness, contrast, and sharpness of this picture have been adjusted in order to emphasize the glow. **d** The ashy plume was from the center of the crater (23 January 2014). This photograph was taken from 3 km west of the crater. **e**, **f** Visible and corresponding infrared thermal images after ash–gas emissions on 13 January 2014. High-temperature (> 550°C) volcanic gas with a minor amount of ash particles was emitted from a vent at the crater center

fluid pathways and the undergoing processes beneath and just off the crater at the time of the activity.

Ash–gas emissions in January 2014 at Aso volcano

In calm periods, the active crater (Nakadake crater) of Aso volcano hosts a hot acidic crater lake (Figs. 1, 2a). The lake is maintained by a balance of incoming and outgoing fluids (Terada et al. 2012). The inlet of the fluid is mainly supplied from deeper regions (more than 90% in both mass and energy), and the effect of precipitation is minor. The amount of hot water in the lake began to decrease in late 2012 and ultimately disappeared in December 2013 (Fig. 2b), probably because of an imbalance in the energy and material budget (Terada and Hashimoto 2017).

After a week of bad weather, a new vent (< 10 m in diameter) was first observed on the crater floor on 2 January 2014 (Fig. 2c). High-temperature gas jets glowed in the vent at night. In tandem with the opening of the new vent, there was an increase in the SO_2 flux discharged from the crater to > 1,000 tons/day (Japan Meteorological Agency 2014), compared to the normal flux of < 300 to 500 tons/day during calm periods (Fig. 3c). However, there was no apparent evidence of ash dispersion associated with this event around the vent on 7 January.

On 13 January, a small amount of ash was first emitted from the vent (Fig. 2d, e), which was estimated to be 100 tons in total (Miyabuchi, Personal Communication, 2014). This amount was more significant than that associated with previous events. For example, less than 40 tons of eruptive mass were ejected during the events that occurred from 2003 to 2005 (Miyabuchi et al. 2008). More than five ash–gas emissions successively occurred from 27 January 2014 until the end of February 2014. We believe that these were phreatomagmatic eruptions, just like the small events that occurred from 2003 to 2005 (Miyabuchi et al. 2008). At approximately the same time in late January, the numbers of long-period (LP) and very-long-period (VLP) events beneath the volcano increased temporarily (Fig. 3a, b; Japan Meteorological Agency 2014). After returning to the normal level, no remarkable seismic activity, except for bursts in July, was observed before the start of the series of the 2014–2015 eruptions on 25 November 2014 (Yokoo and Miyabuchi 2015).

In association with this volcanic activity that preceded the ash–gas emissions in January 2014, we observed an unprecedented and drastic time evolution of tremor amplitude (Fig. 3c). In order to clarify the processes that

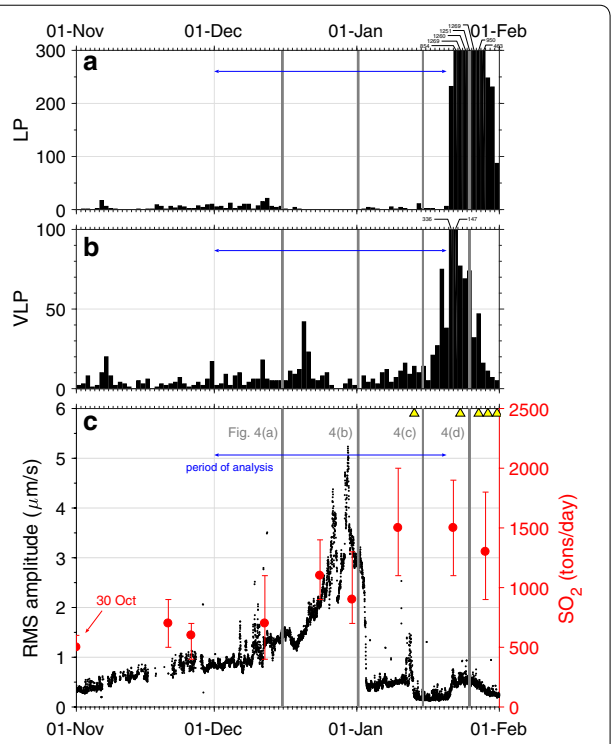

Fig. 3 Seismicity and amplitude variation of volcanic tremors. **a**, **b** Daily numbers of LP and VLP events at Aso volcano for a three-month observation period reported by Japan Meteorological Agency (2014). **c** Change in the root-mean-squared amplitude of the seismic record at SUN (black dots) and SO_2 discharge rate measured by Japan Meteorological Agency (2014) (red circles). The yellow triangles at the top of the diagram represent reported eruptions. Four vertical gray lines that run through (a–c) indicate the times of the graphs shown in Fig. 4. Blue horizontal arrows indicate the time span of our analysis

occurred beneath the crater, we focus on these signals obtained during the two-month period from December 2013 to January 2014 in the following sections.

Data

We used the vertical component of the seismograms recorded at five stations deployed around the active Nakadake crater. Short-period seismometers (Katsushima PK-110V; flat response at 1.5–50 Hz) were installed at three of the stations, SUN, TAK, and KAF (closed circles in Fig. 1b). The other stations, UMAB and KAEB (open circles in Fig. 1b) were equipped with broadband seismometers (Guralp CMG-40T; flat response in 30 s to 50 Hz). The sampling frequency for the seismograms was 100 Hz at all of the stations.

Figure 4 shows 10-min seismograms at SUN and UMAB for four different days in our study period, i.e., 15 December and 1, 15, and 25 January, as indicated in Fig. 3. The upper and middle traces in each diagram show the $>$ 1.5 Hz seismograms at both stations. The $<$ 0.1 Hz waveforms at UMAB are also shown in the bottom trace. There is a significant difference in the amplitude of the $>$ 1.5 Hz signals on the four different days. These high-frequency signals correspond to CTs, as reported by Takagi et al. (2006). According to Takagi et al. (2006, 2009), the frequency of the CTs observed at Aso volcano in 1999 through 2003 was generally high at 3–10 Hz. Similar peak frequencies (2–10 Hz) were observed at stations SUN, TAK, and KAF (Fig. 5a). In contrast, two dominant frequency bands at around 2–4 Hz and 6–12 Hz were observed at KAEB (Fig. 5b). The spectrogram of UMAB was not very clear.

Several types of volcanic seismic signals were always observed at Aso volcano, whether or not the level of volcanic activity was high. For instance, when the CT amplitude was low (Fig. 4c), bursts occurred at 08:26 and 08:32 in the upper two traces. They were attributed to both LP and short-period (SP) events (dominant at 2 and 10 Hz, respectively; Yamamoto 2004; Mori et al. 2008) in association with the VLP events (Mori et al. 2008; Yamamoto et al. 1999) seen in the bottom trace. Identification of these LP and SP events was hampered by the significant CT amplitude (Fig. 4a, b), although larger VLP events occurred at 22:19 on 15 December and at 7:27 on 1 January compared to the 15 January case (Fig. 4c).

We calculated the root-mean-squared (RMS) amplitude of CTs at all stations (frequency: 5–10 Hz; window length: 30 min with an overlap of 50%), and the amplitude ratio between seismic stations pairs for the two-month period of December 2013 to January 2014. For this calculation, we adopted a longer time window than those in previous studies (e.g., Taisne et al. 2011; Ogiso and Yomogida 2012), in order to increase the likelihood that the records were not disturbed by unexpected signals, such as LP and SP events and regional earthquakes. However, we could not completely remove the effects of these earthquakes after 21 January when we observed substantial increases in LP seismicity (Figs. 3a, 4d; Japan Meteorological Agency 2014). We therefore excluded this time period from our analysis.

There are similar amplitude trends in the records for all stations, as shown in Fig. 6a. The SUN data are identical to that calculated from the unfiltered data (Fig. 3c). The amplitude ratio used the SUN data as a reference is shown in Fig. 6b, as an example. Based on the time evolution of the amplitude and the amplitude ratios (Fig. 6), as described below, we divided the analysis period between December 2013 and January 2014 into five stages, labeled I through V.

Stage I The RMS amplitude increased gradually until 22 December. The ratio was approximately constant at all stations. The

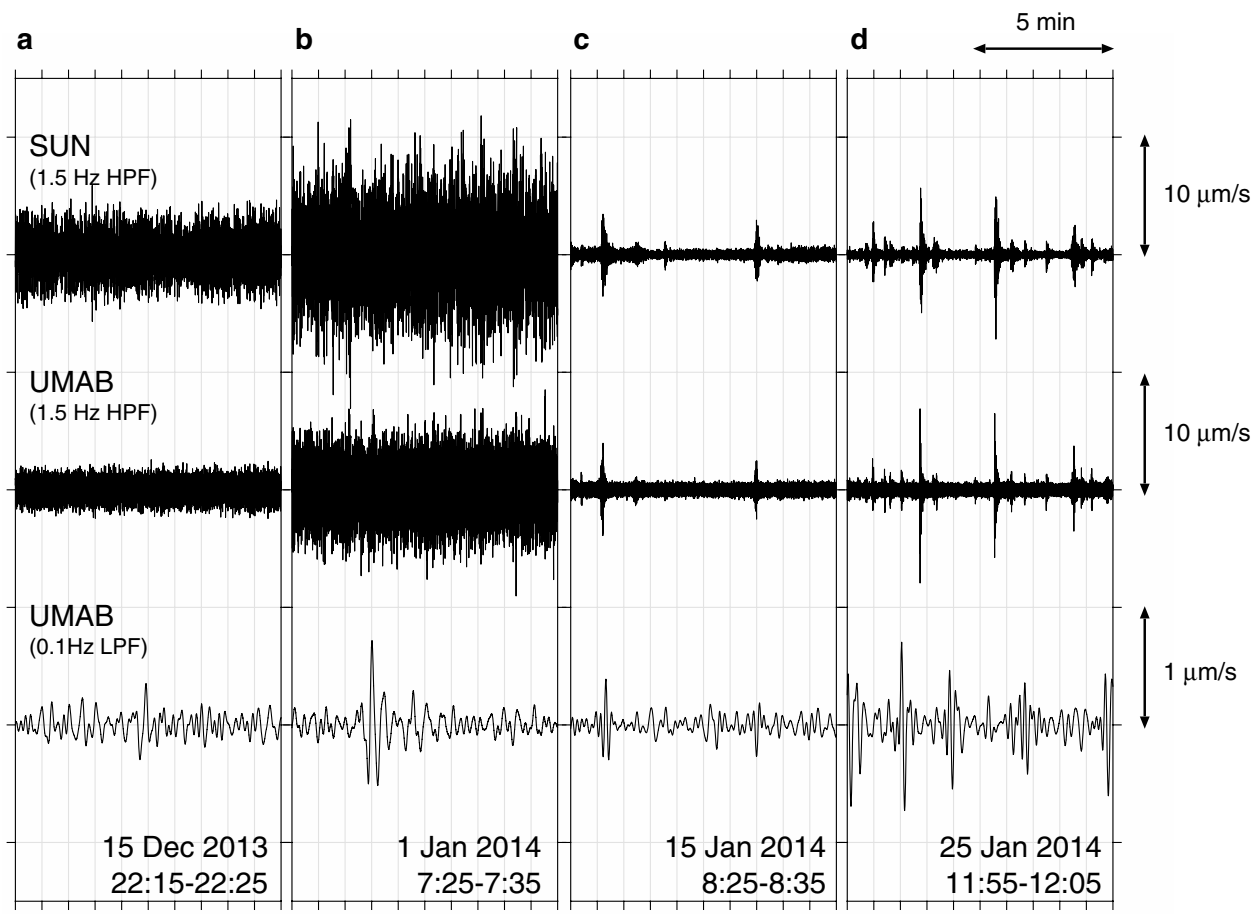

Fig. 4 Waveforms of continuous tremors. Waveforms of continuous tremors recorded at **a** 22:15–22:25 on 15 December 2013, **b** 7:25–7:35 on 1 January 2014, **c** 8:25–8:35 on 15 January 2014, and **d** 11:55–12:05 on 25 January 2014. The traces, from top to bottom, are a 1.5-Hz high-pass vertical seismogram at SUN, a 1.5-Hz high-pass vertical seismogram, and a 0.1-Hz low-pass vertical seismogram at UMAB

amplitude ratios at KAF and KAEB, both of which were closer to the crater (< 500 m away; Fig. 1), were several times larger than those at TAK and UMAB (> 800 m away).

Stage II The amplitude increased rapidly until 29 December. At the end of this phase on 30 December, the RMS amplitude decreased sharply. The amplitude ratio at KAF increased, while that at KAEB decreased. The ratios at UMAB (and probably TAK) were stable, although the TAK values were slightly smaller than that in Stage I.

Stage III The amplitude was stable at a relatively high value for three days and then decreased again on 2–3 January, when the new vent was found (Fig. 2c). No significant difference in the trend of the amplitude ratio from Stage II was observed.

Stage IV Similar to Stage I, a gradual increase in the RMS amplitude was observed. However, on 13 January, when the first ash emission occurred (Fig. 2e, f), a small decrease in amplitude occurred, resulting in the same level as that at the beginning of this stage. The amplitude ratios for both KAF and KAEB were lower compared to those in Stage I. No significant changes could be observed for either TAK or UMAB.

Stage V The RMS amplitudes were relatively steady around their smallest values from 13–20 January. The ratios at both KAF and KAEB became higher and exhibited substantial fluctuations. From the middle to the end of this stage, the ratio at TAK and UMAB began to converge.

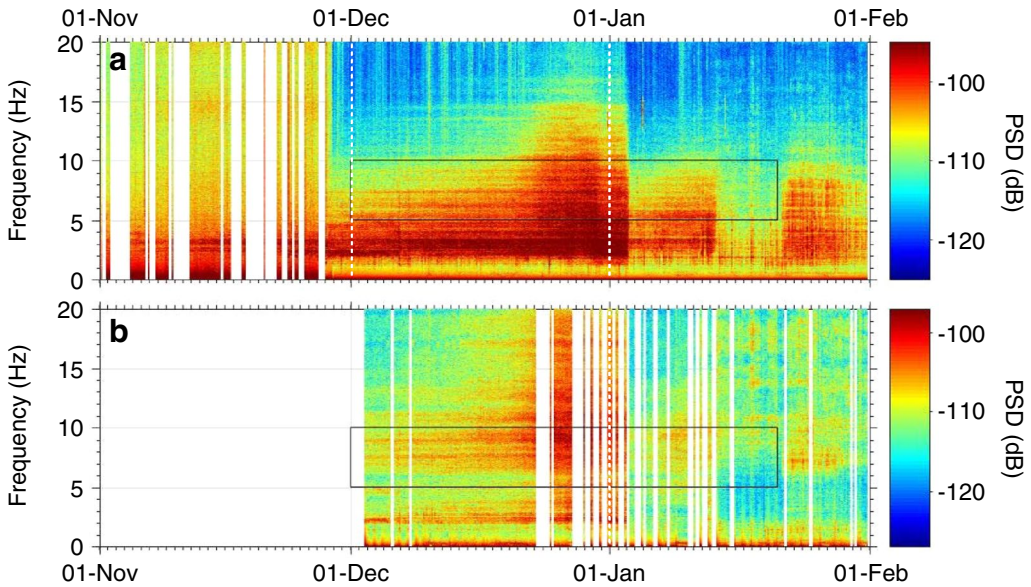

Fig. 5 Spectrograms of continuous tremors. Spectrograms of recorded seismic signals at **a** SUN and **b** KAEB calculated in an eight-hour time window with a four-hour overlap. Data gaps shown in white are caused by, for example, seismometer/digitizer failure or errors in data transmission. Black rectangles spanning from 1 December 2013 to 20 January 2014 at a frequency band of 5–10 Hz indicate the data to be analyzed

Methods

We used the amplitude ratio for locating the source of CTs (Taisne et al. 2011), which is a similar approach to the ASL method (Battaglia and Aki 2003; Kumagai et al. 2010). In the calculation, we assumed that CTs at 5–10 Hz are composed of scattered S-waves, and that they are radiated isotropically from the source. With regard to the first assumption, Kumagai et al. (2010) showed that volcanic tremors are likely to be dominated by S-waves because a large amount of P- to S-wave conversion occurs due to multiple scattering inside volcanoes. Even though we could not identify the exact wave type associated with the observed signals from featureless particle motions, we confirmed that they were not direct P-waves. The second assumption is also due to the highly heterogeneous structure inside volcanoes, which gives rise to a short length of the mean free path for seismic waves, i.e., 100–200 m for 4–16 Hz waves (Shimizu and Ueki 1983; Wegler and Lühr 2001; Wegler 2003; Prudencio et al. 2015). This indicates that seismic waves tend to be scattered shortly after they are produced, which is consistent with the (pseudo-)isotropic radiation pattern for the scattered S-waves.

Under the assumption of isotropic radiation of scattered S-waves, the theoretical amplitude at the i-th station (in m/s; slant distance from a source is r_i km) is expressed as follows (Battaglia and Aki 2003; Kumagai et al. 2010):

$$A_i = A_0 \cdot \frac{1}{r_i} \cdot \exp\left(-\frac{\pi f}{QV} \cdot r_i\right) \cdot S_i,$$

where A_0 is the seismic amplitude at the source (m^2/s), f is the frequency (Hz), Q is the quality factor, V is the S-wave velocity (km/s), and S_i is the site amplification factor described in the next paragraph. The tremor amplitude ratio between the i-th station and the j-th station is

$$\begin{aligned} A'_{ij} &= A_i/A_j \\ &= \frac{r_j}{r_i} \cdot \exp\left(-\frac{\pi f}{QV} \cdot (r_i - r_j)\right) \cdot \frac{S_i}{S_j}. \end{aligned}$$

This amplitude ratio is only a function of the source-station distance r when we fix the other parameters. We choose $f = 7.5$ Hz (corresponding to 5- to 10-Hz band data), $Q = 50$ (Sudo 1991), and $V = 1.12$ km/s (calculated from the P-wave velocity (1.91 km/s) and the P- to S-wave velocity ratio (1.704) Sudo and Kong 2001; Sudo et al. 2002).

The site amplification factor S_i was calculated by the coda normalization method (Phillips and Aki 1986). We selected 153 earthquakes listed in a catalog of the Japan Meteorological Agency ($M \geq 2.0$; from May 2011 to June 2012). Their hypocentral distances were 10–200

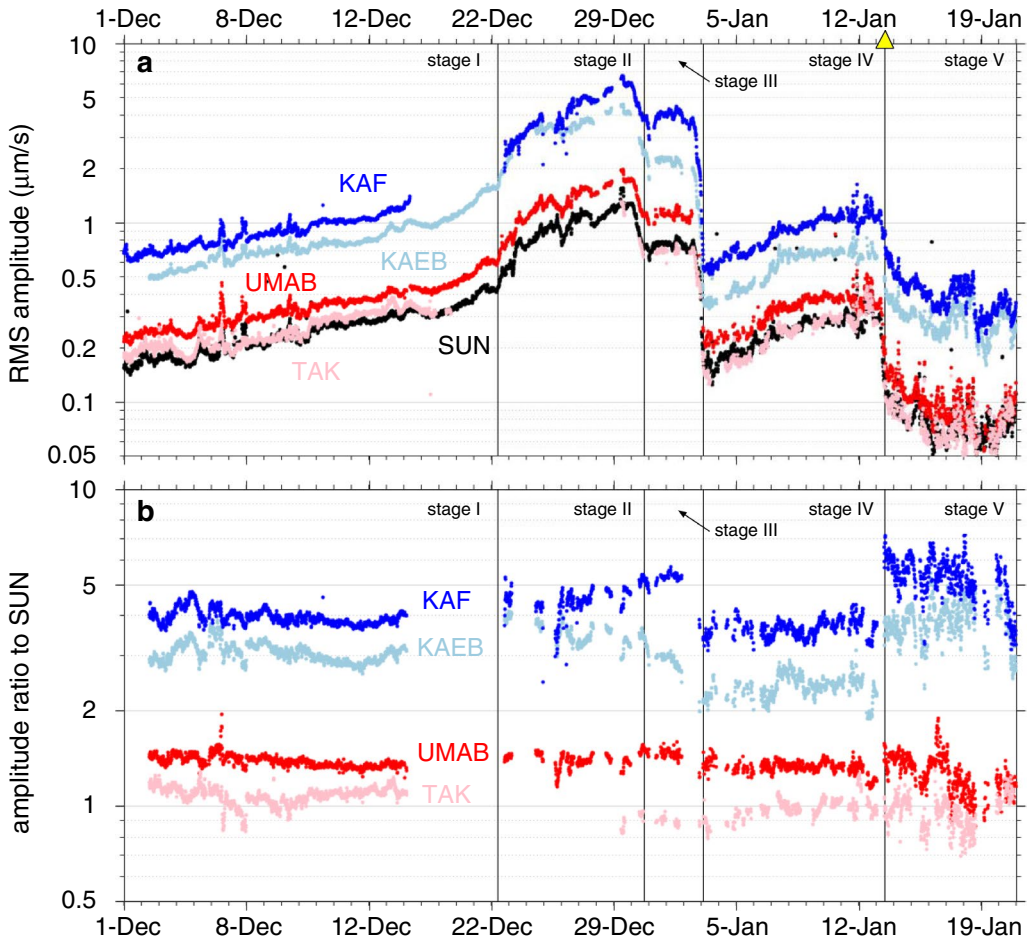

Fig. 6 Observed root-mean-squared amplitude and amplitude ratio. **a** Time evolution of root-mean-squared amplitude recorded at all stations (frequency: 5–10 Hz; window length: 30 min with a sliding length of 15 min). The yellow triangle represents the reported eruption (Japan Meteorological Agency 2014). The boundaries of the five stages defined in the present study are shown as vertical lines. **b** Examples of amplitude ratios at each station (in this case, referenced to SUN)

Table 1 Site amplification factors referenced to SUN

	TAK	KAF	UMAB	KAEB
Site amplification factor	1.118	0.919	0.959	1.309
Standard deviation	0.191	0.223	0.236	0.329
Numbers of analyzed seismic events	95	63	88	77

km from Aso volcano, and their back azimuths were equally distributed in all directions. According to Ogiso and Yomogida (2012, 2015), we used 5- to 10-Hz band-passed seismograms in a 10-s time window twice after the arrival of the S-wave. The S-wave travel times were calculated using the table of Ueno et al. (2002). Table 1 shows the results of the calculations in the form of a ratio based on that for the SUN station.

To locate the CT sources, a three-dimensional grid search using the observed amplitude ratio A'^{obs}_{ij} was applied so as to minimize the normalized residual ϵ:

$$\epsilon = \frac{100}{N_p}\sqrt{\frac{\sum_{i,j}\left(A'_{ij} - A'^{\mathrm{obs}}_{ij}\right)^2}{\sum_{i,j}\left(A'^{\mathrm{obs}}_{ij}\right)^2}},$$

where N_p is the number of station pairs. In the present study, we chose four or five stations to be used, so that N_p was 6 or 10. We regarded the grid point at which the normalized residual took a minimum value ($\epsilon_{\mathrm{min}} \leq 1.67$) as the CT source location. The threshold value of ϵ_{min} that we chose was equivalent to the error level in Jones et al. (2013), who examined the validity of the ASL method by comparing the locations of known seismic sources (shots) and inverted locations using the amplitudes

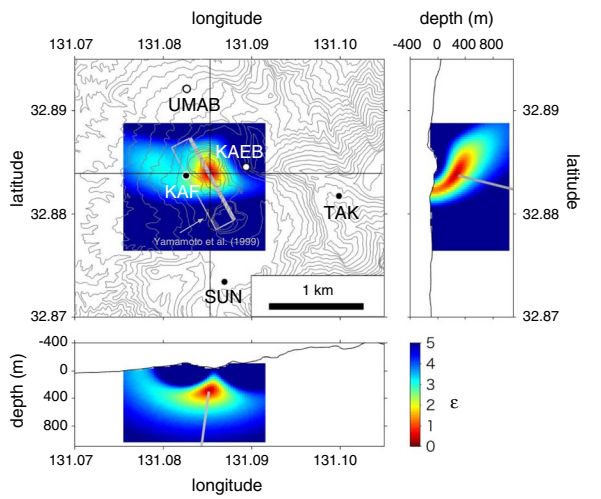

Fig. 7 Example distribution of the computed residual for source estimation. Distribution of the calculated normalized residual ϵ at 13:00 on 15 December 2013. In the map view, the estimated source location of continuous tremors is situated inside the crater, where two black lines cross. The cross sections in the NS and EW directions are along these lines. The crack-like conduit in which the source of repeated VLP events proposed by Yamamoto et al. (1999) is also shown by the gray rectangle and lines in the map and the cross sections, respectively

at six stations. The grid search region was 1500 m (N-S) × 1500 m (E-W) × 1200 m (depth) around the crater, with a 25-m increment in all directions.

Results

An example of our CT source estimation results is shown in Fig. 7, where we used the data in Stage I (13:00 on 15 December 2013). The estimated source location is at a depth of 200 m beneath the crater ($\epsilon_{\min} = 1.08$). This corresponds to the upper end of the crack-like conduit, where repeated VLP events usually occur (Yamamoto et al. 1999). The residual pattern in the NS cross section extends more widely than that in EW cross section. This pattern is due to the limited distribution of our five seismic stations (Figs. 1, 7), suggesting that it would be better for more precise source location to place at least one more station between the crater and either SUN or UMAB.

During the two-month period from December 2013 to January 2014, we estimated the source location of CTs every 15 min. The time evolution of both the depth and the horizontal position are compiled in Fig. 8. To plot the horizontal position, we used components both parallel and perpendicular to the strike direction of the crack, N28°W (Fig. 7; Yamamoto et al. 1999). In the following, we refer to these components as the NS and EW components, respectively. The source is situated consistently at a depth of 200 m throughout Stages I to III. However, in Stage IV, the source depth suddenly drops to 400 m and then gradually returns to ∼ 200 m. During Stage V, the source position fluctuates within the shallowest depth of 0–200 m. The estimated source position in a map view is, on the whole, ∼ 100 m southwest from the center of the

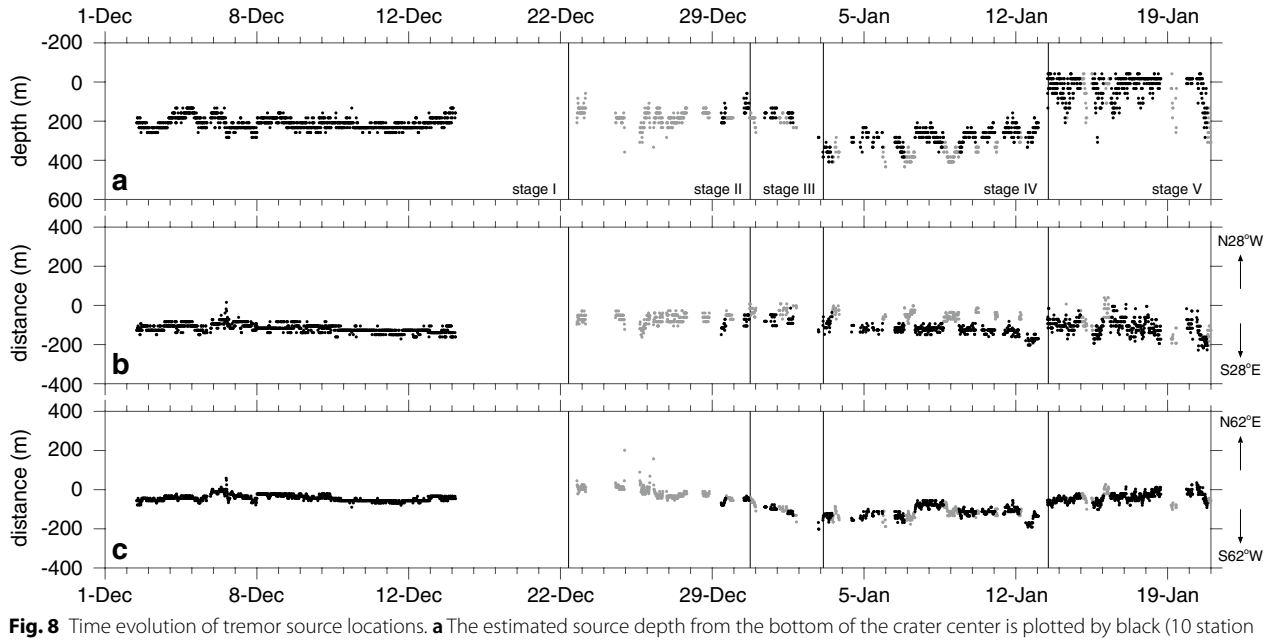

Fig. 8 Time evolution of tremor source locations. **a** The estimated source depth from the bottom of the crater center is plotted by black (10 station pairs) and gray (six station pairs) dots. The four vertical lines represent the boundaries between each stage. **b**, **c** The horizontal locations are plotted in parallel and perpendicular to the strike direction of the crack (Yamamoto et al. 1999). The zero indicates the crater center

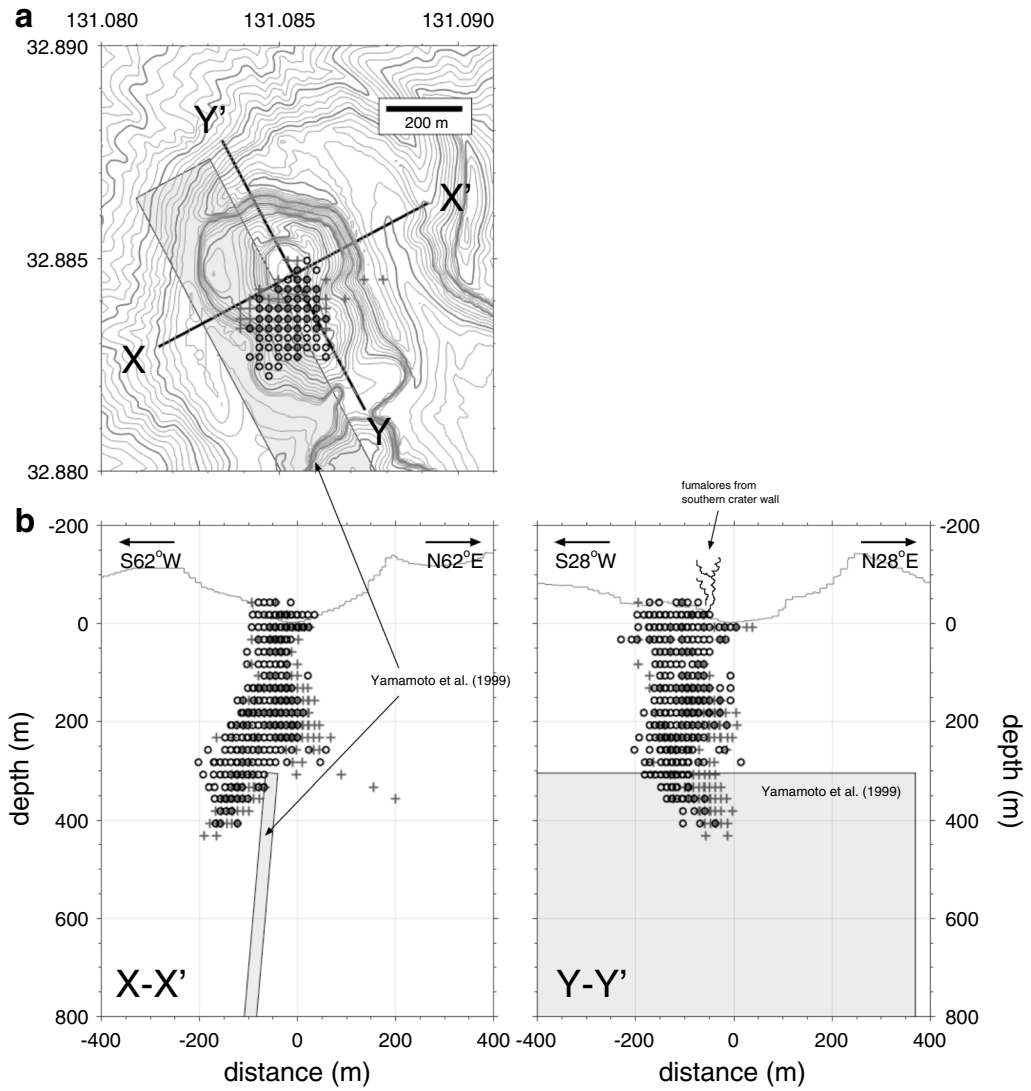

Fig. 9 Distribution of source locations of continuous tremors. Distribution of the source locations of continuous tremors for all stages plotted in **a** map view and **b** cross sections based on Fig. 8a–c. The black circles and gray crosses are the results estimated using ten and six station pairs, respectively. The intersection of lines X-X' and Y-Y' indicates the center of the crater. Gray shaded areas represent the crack proposed by Yamamoto et al. (1999)

crater (Fig. 9a). Although westward, and then eastward shifting occurs during Stages II through III and Stages IV through V, respectively, the horizontal location is more stable to within ±160 m in the NS component (Fig. 8b) and ±120 m in the EW component (Fig. 8c). For all stages of the analyzed period, the estimated CT source locations are likely to be distributed in an inclined roughly cylindrical region beneath the crater (Fig. 9). Most of these locations are situated above the top portion of the crack reported by Yamamoto et al. (1999). No significant differences between the number of station pairs (6 or 10) used for the calculation were found (Fig. 8).

Discussion

In the present study, we located the CT sources at Aso volcano in the period from December 2013 to January 2014 using the seismic amplitude records from five stations (Fig. 1). We found that the sources were distributed from the surface to a depth of ∼ 400 m beneath the active crater (Fig. 9). Migration of the sources could also be identified in the analyzed period (Fig. 8). In this section, from the spatiotemporal distribution of these source locations, we briefly discuss a pathway for the volcanic fluids at Aso volcano and the source processes beneath the crater from 2013 to 2014.

Our result shows that the CT sources were apparently distributed beneath the active crater (Fig. 9). However, the horizontal position was ~ 100 m south of the center of the crater. We consider that this offset is valid because it is consistent with the results of an array analysis of CTs (Takagi et al. 2006, 2009). A fumarolic zone at the southern crater wall (Fig. 2a) might also be evidence of this offset. Moreover, we found that the sources extended from the ground surface to a depth of ~ 400 m. The source locations appear to be confined within a region with an inclined roughly cylindrical shape (Fig. 10). Assuming this to be the case, we approximated the diameter at different depths based on the cross-sectional area. The cross-sectional circular area was estimated by summing the different source grids (25×25 m^2 each). The resulting diameter was 100–150 m, and there was no significant change with depth (Fig. 10a). By connecting the epicenters of these circles, the dip angle of the cylindrical region was found to be 80.7°. The lower part of the cylindrical source region coincides with the uppermost portion of the large crack-like conduit (2.5 km in length and 1.0 km in width) reported by Yamamoto et al. (1999) where repeated VLP events occur (Figs. 3, 4). The estimated dip angle for the CT source ~ 81° is practically the same as that for the crack (85°), which implies that the CT source is closely related to the existing crack.

According to the model proposed by Yamamoto (2004) and Yamamoto et al. (1999), the large crack situated beneath the CT sources is part of a transportation system of gas-dominated volcanic fluid. The fluid flows upwards toward the crater, probably from the magma reservoir situated at a depth of 6 km (Sudo and Kong 2001; Nobile et al. 2017). Therefore, we believe that most of the shallow CT source regions lie in the final section of the fluid pathway to the crater. Before approaching the crater, the volcanic fluid at the top portion of the crack may flow horizontally and become concentrated near the central region, despite a deviation of ~ 100 m from the crater center (Figs. 9a, 10e).

We believe that this region of the pathway consists of complex plexus structures, and perhaps networks of fractures with different sizes. This is consistent with the

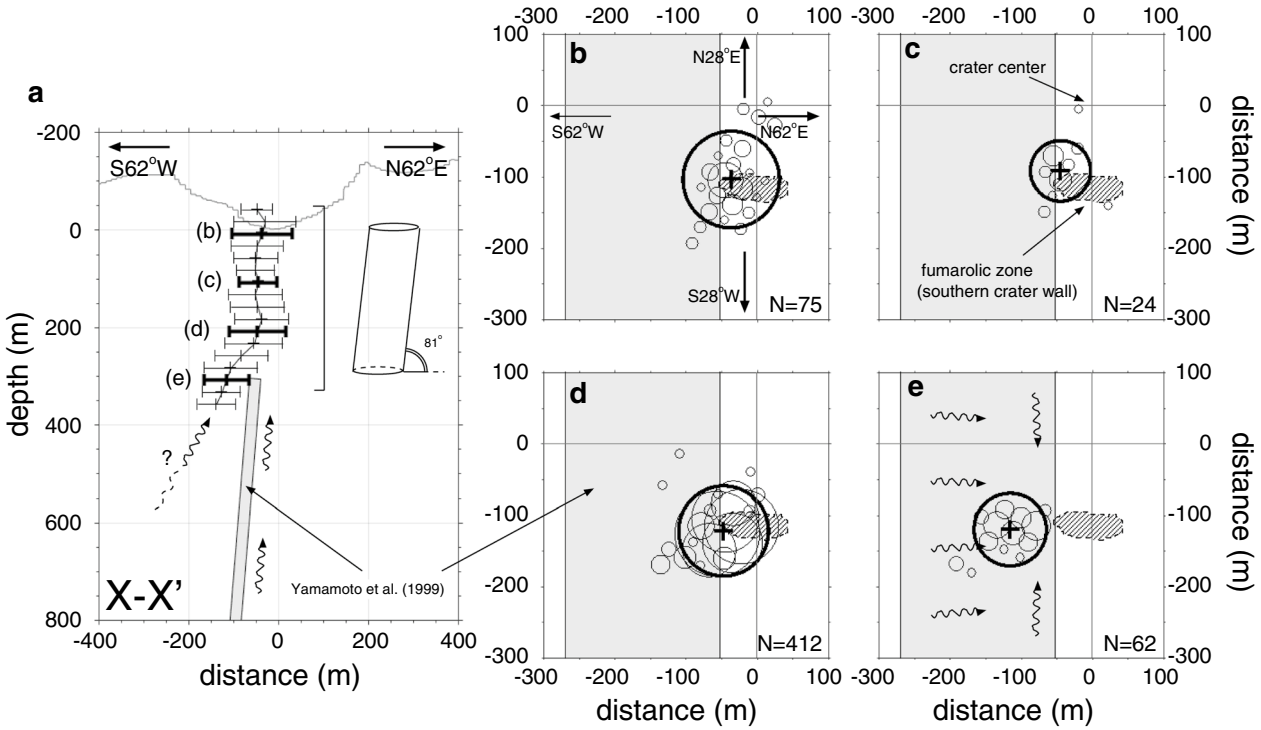

Fig. 10 The region containing the sources of the continuous tremors is an inclined cylinder. **a** Weighted centroid of estimated CT source locations ($N_p = 10$; black circles in Fig. 9) at each depth with a disk size (horizontal bar). The results are projected on a vertical plane perpendicular to the strike direction of the crack (gray area; Yamamoto et al. 1999). The distribution of these disks consists of an inclined cylindrical region (dip is 80.7°; inserted sketch). Wiggly lines indicate the flow direction of the volcanic fluid. **b**–**e** Horizontal distribution of both the apparent disk area of the cylindrical region (thick circle) and all estimated source locations (thin circles) at depths of 0, 100, 200, and 300 m, respectively. The size of each thin circle indicates the number of crossovers. The total number of source estimations (30-min windows) is shown in the lower right. The hatched area corresponds to a fumarolic zone at the southern crater wall (Fig. 2). The wiggly lines in **e** show the flow directions not only at a depth of 300 m, but also in the entire region of the crack

results obtained by an AMT survey (Kanda et al. 2008), in which a low-resistivity region (10^0 to $10^{0.5}$ Ωm) was observed at depths of 0–400 m beneath the crater. High-temperature volcanic fluid (dominated by magmatic gas) infiltrates the sedimentary rocks because of their high permeability, which likely causes a decrease in the resistivity of the rocks (Komori et al. 2010). The diameter of 100–150 m for the roughly cylindrical pathway is approximately equal to that of the actual crater floor (Fig. 9a), whose area was estimated to be $\sim 1 \times 10^4$ m^2 based on digital surface modeling performed in 2007 (Terada et al. 2008). This coincidence in size suggests that the fluid supply to the volcanic lake can occur by seepage from the entire area of the crater bottom, whether or not the primary pathway, similar to the vent observed in January 2013 (Fig. 2c–e), is open. This is supported by the fact that several water remnants and steaming areas were distributed over the entire crater floor when most of the lake water had disappeared (Fig. 2b).

Some studies have associated source processes with the generation of volcanic tremors (e.g., Chouet 1988; Iwamura and Kaneshima 2005; Neuberg et al. 2005). However, tremors are often thought to be related to the movement of volcanic fluids (magma and gas) through pathways such as conduits, dikes, and fissures. Julian (1994) proposed a simple theoretical model of the tremor in which fluid movement in a channel causes oscillation of the elastic walls of the path. A similar process with tremor-like seismic signatures has been reproduced in laboratory experiments on rock deformation (Benson et al. 2008; Burlini et al. 2007). Based on the results, tremors can occur when fluids move into the preexisting crack or fracture networks that have newly resulted from rock failure. The observed complex shape of the pathways in the specimen is also responsible for tremor generation, as postulated in the literature (Julian 1994). Following these models, we consider that movement of fluid related to volcanic gas could generate the CTs observed during the analysis period.

To investigate the processes of fluid migration at Aso volcano from 2013 to 2014, in addition to analyzing the CT source locations (Fig. 8), we derived the source amplitude $\overline{A_0}$ in 15-min time windows using the following equation:

$$\overline{A_0} = \frac{1}{N_s} \sum_i \left(\frac{r_i A_i^{\mathrm{obs}}}{S_i} \cdot \exp\left(\frac{\pi f}{QV} \cdot r_i \right) \right),$$

where N_s is the number of stations, which is assumed to be four or five in our case. The results of this estimation are shown in Fig. 11. The trend of the source amplitude during the two-month period is quite similar to the observed RMS amplitude at the stations (Fig. 6a). We consider that these changes are strongly reflected in the actual progression of volcanic processes beneath

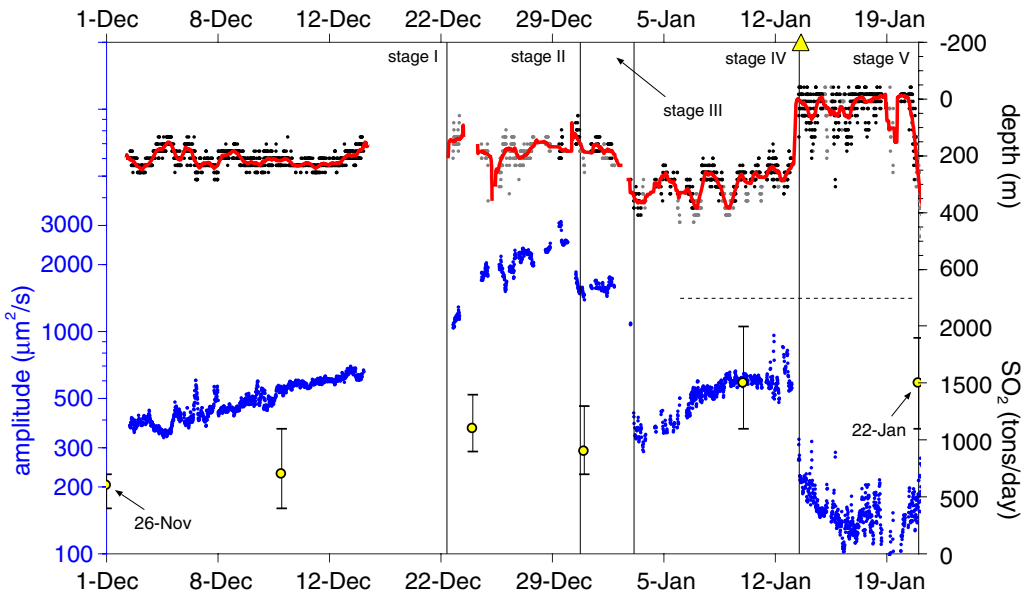

Fig. 11 Time evolution of the source amplitude and the depth of continuous tremors. The estimated source amplitude $\overline{A_0}$ (blue dots) and source depth (black and gray dots; as in Fig. 8a) are plotted with respect to time. The red lines show the 24-hour moving average of the depth data. SO_2 discharge rate is also potted again by yellow circles (Japan Meteorological Agency 2014). The yellow triangle at the top of the diagram indicates the reported eruption (Japan Meteorological Agency 2014)

the crater. The increase in the source amplitude during Stages I through III is thought to be related to an increase in the flow of volcanic fluid toward the opening of the eruption vent. At these times, we actually observed an increase in the SO_2 discharge rate (Figs. 3c, 11). Since the upward fluid supply increased, the pathways might have expanded in order to accommodate the higher flux. On the other hand, after the opening of the vent (Stages IV and V), the source amplitude decreased in a stepwise manner to a low level (Fig. 11). However, the SO_2 discharge rate remained quite high at $\sim 1,500$ tons/day, which was evidence that transport pathways for the volcanic fluid had been established, so that no significant source amplitude could be estimated.

The results of the present study allow us to interpret sequential processes beneath the active crater of Aso volcano leading up to the ash–gas emissions in January 2014 in association with volcanic fluid migration. They can be summarized as follows.

Stage I In this stage, the amount of gas-dominated volcanic fluid transported from depth to the crater had gradually increased as compared to that in the period before analysis. This supply of the fluid led to an expansion of the zone of fluid pathways (probably aggregation of fractures) especially in a shallow portion (depth: ~ 200 m) between the crater floor and the upper edge of the crack-like conduit (Fig. 11). We could observe this process of CT generation with a gradual increase in amplitude. The rise of fluid supply is also indicated by a continuation of the gradual increase in the SO_2 discharge rate (Figs. 3c and 11).

Stage II A more considerable amount of fluid was supplied to the system. SO_2 degassing continued to increase and achieved a high level of $\sim 1,000$ tons/day (Figs. 3c, 11). This supply caused the entire pathway area to expand further, which may explain why the increase in the CT amplitude became more significant at this stage (Fig. 11). No change in the source depth of around 100 to 300 m was evident. At the end of this stage, we observed a sharp decrease in the amplitude, which suggests that stresses associated with fluid flows became too low. This decrease in amplitude could occur when the size of the pathway becomes sufficient to transport the fluid therein. We infer that the vent, i.e., the exit of the pathway, may have indeed opened on 30 December 2013 although a new vent was first observed on 2 January 2014 after bad weather conditions (Fig. 2c; at the end of Stage III).

Stage III We observed that the tremor amplitude remained at a higher level and the estimated source depth was approximately the same as that in Stage II (Fig. 11). Therefore, we consider that the pathway area was still enlarging in order to transport the fluid in a manner similar to Stage II. At the end of this stage, the path system for the volcanic fluid beneath the crater was wholly established. The vent size was enlarged to < 10 m (Fig. 2c), which again led to a sharp decrease in the tremor amplitude (Fig. 11) although a high level of SO_2 degassing was still observed (Figs. 3c, 11).

Stage IV The highest SO_2 discharge rate of 1500 tons/day was recorded during this period (Figs. 3c, 11), which indicates that a significant amount of volcanic fluid was still being supplied from below. Since the first ash–gas emission (100 tons of ash; Miyabuchi, Personal Communication, 2014) occurred on 13 January (Fig. 2e), at the end of this stage, we consider that the fluid was more magmatic than in previous stages. From this viewpoint, the CT source location may be noteworthy, in that the source depth (200–400 m; Fig. 11) evidently coincided with the uppermost part of the crack. However, there was some lateral divergence from the crack (Fig. 9b), and the source depth shows apparent upward migration with some back and forth fluctuations (Fig. 11). In order to explain these results, one possible scenario is that a process forming a new route for the volcanic fluid leading to the 13 January event occurred just beside the existing crack (west side) (Fig. 10). A phenomenon similar to a tremor, cyclic forward and backward migration, was recorded in association with a dike propagation (Caudron et al. 2018). At Aso volcano, no different VLP events were observed even when magmatic eruptions occurred (Sandanbata et al. 2015), and those during periods with a sustained crater lake. This suggests that there are several (isolated) pathways beneath the crater (one is for magmatic fluid without

VLP events, i.e., the new west route; and the other is for a great deal of gaseous fluid related to repeated VLP events, i.e., the crack). At a depth of < 200 m above the confluence point between these pathways, the fluid path was already large enough to accommodate the fluid for the 13 January event. This is the reason why no CT source location was determined before the eruption. However, we cannot precisely explain why this kind of process to form a new pathway did not generate a significant CT amplitude, as in Stages II and III (Fig. 11). A more accurate picture of the conduit system of Aso volcano should also be obtained. Once the ash–gas emission occurred at the end of this stage, the pressure decreased in the pathway and thus the tremor amplitude decreased to the background level (Fig. 11).

Stage V During this stage, from 13 to 20 January, the tremor amplitude was significantly small (Fig. 11). The spectral character of the recorded signals was somewhat different from that in the previous stages (Fig. 5). This indicates that the seismograms in this stage did not include particular CT signals and were likely composed of signals associated with strong gas jetting from the vent (McKee et al. 2017). Detection of gas jetting is why the source locations were determined to be at much shallower depths around the ground surface (Fig. 11). An open conduit system maintained the highest SO_2 discharge rate of ~ 1500 tons/day (Figs. 3c, 11). Since the conduit system had been established, subsequent ash–gas emissions smoothly occurred in more than five events during the next ten days (Japan Meteorological Agency 2014).

Based on the results of analysis on the CTs, we clarified the pathway distribution for the volcanic fluid beneath the crater at Aso volcano. We also showed that the location of CT sources is undoubtedly crucial in capturing subsurface processes concerning fluid migration and so must be monitored. A similar increase in tremor activities to this 2013–2014 event has been observed at Aso volcano on several instances, before the small ash–gas emission in 2011, during the series of magmatic eruptions in 2014–2015, and before some phreatic and phreatomagmatic explosions in 2016. In order to clarify the causal relationship between the conduit process and CT, further analyses of these events are required. An improved understanding of the fluid transport processes in shallow conduit systems at the volcano may lead to more effective hazard mitigation.

Conclusion

We estimated the source locations of continuous tremors at Aso volcano over a two-month period preceding ash–gas emissions in January 2014. We used temporal variations in the seismic amplitude ratio observed at just five stations around the active crater. The sources were estimated to be distributed from the ground surface to a depth of 400 m beneath the crater. We infer that the tremor source area is a region of fracture networks in which gas-dominated volcanic fluid is always transported to the crater in order to sustain the crater lake. This gas-dominated fluid is supplied from a deep area through a large crack that exists just beneath the source region of the tremors. The estimated source locations for the continuous tremors were also found to migrate in association with surficial volcanic activity. In particular, during the ten-day period leading up to the start of the ash–gas emissions (small phreatomagmatic eruptions), the sources were situated at the deepest position during the analysis period and beside the crack position. We speculated that this spatial discrepancy between the source locations and the crack might be caused by the formation of new pathways by more magmatic fluid supplied directly from the magma chamber. Based on the results of the present study, we found that signals associated with continuous tremors related to the eruptive activity have the potential to be used to interpret the fluid dynamics inside a volcano. Therefore, from the standpoint of eruption forecasting, continuous tremors should be carefully monitored to track their source locations, especially when new pathways have been established.

Authors' contributions

MI performed all the analysis in the present study. AY, MI, and TK contributed to the planning, data analysis, and interpretation of the present study. SY and HI participated in the acquisition of seismic data. All authors read and approved the final manuscript.

Author details

[1] Department of Geophysics, Graduate School of Science, Kyoto University, Kitashirakawa Oiwake-cho, Sakyo-ku, Kyoto 606-8502, Japan. [2] Present Address: Geospatial Information Authority of Japan, Tsukuba, Japan. [3] Aso Volcanological Laboratory, Institute for Geothermal Sciences, Kyoto University, 3028 Sakanashi, Aso, Kumamoto 869-2611, Japan.

Acknowledgements

The authors would like to thank T. Ohkura for providing the seismic data used in the present study and M. Yamamoto for providing valuable advice and comments. Comments from two anonymous reviewers and the editor, Dr. V. Acocella, greatly improved the manuscript.

Competing interests
The authors declare that they have no competing interests.

Availability of data and materials
The data that support the findings of the present study are available from the corresponding author upon a request.

Funding
The present study was financially supported by Ministry of Education, Culture, Sports, Science and Technology of Japan under its Earthquake and Volcano Hazards Observation and Research Program and by a Grant-in-Aid for Young Scientists (No. 25870352 for AY).

Publisher's Note

Received: 22 February 2018 Accepted: 26 July 2018
Published online: 03 August 2018

References

Almendros J, Ibáñes JM, Carmona E, Zandomeneghi D (2007) Array analyses of volcanic earthquakes and tremor recorded at Las Cañadas caldera (Tenerife Island, Spain) during the 2004 seismic activation of Teide volcano. J Volcanol Geotherm Res 160(3–4):285–299. https://doi.org/10.1016/j.jvolgeores.2006.10.002

Battaglia J, Aki K (2003) Location of seismic events and eruptive fissures on the Piton de la Fournaise volcano using seismic amplitude. J Geophys Res 108(B8):2364. https://doi.org/10.1029/2002JB002193

Benson PM, Vinciguerra S, Meredith PG, Young RP (2008) Laboratory simulation of volcano seismicity. Science 322:249–252. https://doi.org/10.1126/science.1161927

Burlini L, Vinciguerra S, Di Toro G, De Natale G, Meredith P, Burg JP (2007) Seismicity preceding volcanic eruptions: new experimental insights. Geology 35(2):183–186. https://doi.org/10.1130/G23195A.1

Caudron C, White RS, Green RG, Woods J, Ágústsdóttir T, Donaldson C, Greenfield T, Rivalta E, Brandsdóttir B (2018) Seismic amplitude ratio analysis of the 2014–2015 Bárðarbunga-Holuhraun dike propagation and eruption. J Geophys Res 123:264–276. https://doi.org/10.1002/2017JB014660

Chouet B (1988) Resonance of a fluid-driven crack: Radiation properties and implications for the source of long-period events and harmonic tremor. J Geophys Res 93(B5):4375–4400. https://doi.org/10.1029/JB093iB05p04375

Iwamura K, Kaneshima S (2005) Numerical simulation of the steam-water flow instability as a mechanism of long-period ground vibrations at geothermal areas. Geophys J Int 163(2):833–851. https://doi.org/10.1111/j.1365-246X.2005.02749.x

Japan Meteorological Agency (2014) Monthly Volcanic Activity Report (2014). http://www.data.jma.go.jp/svd/vois/data/tokyo/STOCK/monthly_v-act_doc/fukuoka/14m01/503_14m01.pdf

Jones GA, Kulessa B, Doyle SH, Dow CF, Hubbard A (2013) An automated approach to the location of icequakes using seismic waveform amplitudes. Ann Glaciol 54(64):1–9. https://doi.org/10.3189/2013AoG64A074

Julian BR (1994) Volcanic tremor: nonlinear excitation by fluid flow. J Goephys Res 99(B6):11,859–11,877. https://doi.org/10.1029/93JB03129

Kanda W, Tanaka Y, Utsugi M, Takakura S, Hashimoto T, Inoue H (2008) A preparation zone for volcanic explosions beneath Naka-dake crater, Aso volcano, as inferred from magnetotelluric surveys. J Volcanol Geotherm Res 178(1):32–45. https://doi.org/10.1016/j.jvolgeores.2008.01.022

Komori S, Kagiyama T, Hoshizumi H, Takakura S, Mimura M (2010) Vertical mapping of hydrothermal fluids and alteration from bulk conductivity: simple interpretation on the USDP-1 site, Unzen Volcano, SW Japan. J Volcanol Geotherm Res 198(3–4):339–347. https://doi.org/10.1016/j.jvolgeores.2010.09.019

Kumagai H, Nakano M, Maeda T, Yepes H, Palacios P, Ruiz M, Arrais S, Vaca M, Molina I, Yamashina T (2010) Broadband seismic monitoring of active volcanoes using deterministic and stochastic approaches. J Geophys Res 115(B8):B08303. https://doi.org/10.1029/2009JB006889

McKee K, Fee D, Yokoo A, Matoza RS, Kim K (2017) Analysis of gas jetting and fumarole acoustics at Aso Volcano, Japan. J Volcanol Geotherm Res 340:16–29. https://doi.org/10.1016/j.jvolgeores.2017.03.029

McNutt SR (1992) Volcanic tremor. In: Nierenberg WA (ed) Encyclopedia of earth system science. Academic Press, San Diego, pp 417–425

Miyabuchi Y, Ikebe S, Watanabe K (2008) Geological constraints on the 2003–2005 ash emissions from the Nakadake crater lake, Aso Volcano. Japan. J Volcanol Geotherm Res 178(2):169–183. https://doi.org/10.1016/j.jvolgeores.2008.06.025

Mori T, Sudo Y, Tsutusi T, Yoshikawa S (2008) Characteristics of isolated hybrid tremor (HBT) during a calm activity period at Aso volcano. Bull Volcanol 70(9):1031–1042. https://doi.org/10.1007/s00445-007-0185-7

Morioka H, Kumagai H, Maeda T (2017) Theoretical basis of the amplitude source location method for volcano-seismic signals. J Goephys Res 122(8):6538–6551. https://doi.org/10.1002/2017JB013997

Neuberg JW, Tuffen H, Colliera L, Green D, Powell T, Dingwell D (2005) The trigger mechanism of low-frequency earthquakes on Montserrat. J Volcanol Geotherm Res 153(1–2):37–50. https://doi.org/10.1016/j.jvolgeores.2005.08.008

Nobile A, Acocella V, Ruch J, Aoki Y, Borgstrom S, Siniscalchi V, Geshi N (2017) Steady subsidence of a repeatedly erupting caldera through InSAR observations: Aso, Japan. Bull Volcanol 79(5):32. https://doi.org/10.1007/s00445-017-1112-1

Ogiso M, Yomogida K (2012) Migration of tremor locations before the 2008 eruption of Meakandake Volcano, Hokkaido, Japan. J Volcanol Geotherm Res 217–218:8–20. https://doi.org/10.1016/j.jvolgeores.2011.12.005

Ogiso M, Yomogida K (2015) Estimation of locations and migration of debris flows on Izu-Oshima Island, Japan, on 16 October 2013 by the distribution of high frequency seismic amplitudes. J Volcanol Geotherm Res 298:15–26. https://doi.org/10.1016/j.jvolgeores.2015.03.015

Patanè D, Grazia D, Cannata A, Montalto P, Boschi E (2008) Shallow magma pathway geometry at Mt. Etna volcano. Geochem Geophys Geosyst 9(12):Q12021. https://doi.org/10.1029/2008GC002131

Phillips WS, Aki K (1986) Site amplification of coda waves from local earthquakes in central California. Bull Seismol Soc Am 76(3):627–648

Prudencio J, Del Pezzo E, Ibáñes JM, Giampiccolo E, Patané D (2015) Two-dimensional seismic attenuation images of Stromboli Island using active data. Geophys Res Lett 42:1717–1724. https://doi.org/10.1002/2015GL063293

Sandanbata O, Obara K, Maeda T, Takagi R, Satake K (2015) Sudden changes in the amplitude-frequency distribution of long-period tremors at Aso volcano, southwest Japan. J Geophys Res 42:10,256–10,262. https://doi.org/10.1002/2015GL066443

Shimizu H, Ueki S (1983) Application of diffusion theory to seismograms of volcanic earthquakes [abstract]. Bull Volcanol Soc Jpn 28(2):196–197

Sudo Y (1991) An attenuating structure beneath the Aso Caldera determined from the propagation of seismic waves. Bull Volcanol 53:99–111. https://doi.org/10.1007/BF00265415

Sudo Y, 89 persons, (2002) 1998 seismic exploration, Aso98, in Aso Volcano. Bull Earthq Res Inst 77:303–336

Sudo Y, Kong L (2001) Three-dimensional seismic velocity structure beneath Aso Volcano, Kyushu. Japan. Bull Volcanol 63(5):326–344. https://doi.org/10.1007/s004450100145

Taisne B, Brenguier F, Shapiro NM, Ferrazzini V (2011) Imaging the dynamics of magma propagation using radiated seismic intensity. Geophys Res Lett 38(4):L04304. https://doi.org/10.1029/2010GL046068

Takagi N, Kaneshima S, Kawakatsu H, Yamamoto M, Sudo Y, Ohkura T, Yoshikawa S, Mori T (2006) Apparent migration of tremor source synchronized with the change in tremor amplitude observed at Aso volcano. Japan. J Volcanol Geotherm Res 154(3–4):181–200. https://doi.org/10.1016/j.jvolgeores.2006.02.001

Takagi N, Kaneshima S, Ohkura T, Yamamoto M, Kawakatsu H (2009) Long-term variation of the shallow tremor sources at Aso Volcano from 1999 to 2003. J Volcanol Geotherm Res 184(3–4):333–346. https://doi.org/10.1016/j.jvolgeores.2009.04.013

Terada A, Hashimoto T (2017) Variety and sustainability of volcanic lakes: Response to subaqueous thermal activity predicted by a numerical model. J Geophys Res 122(8):6108–6130. https://doi.org/10.1002/2017JB014387

Terada A, Hashimoto T, Kagiyama T, Sasaki H (2008) Precise remote-monitoring technique of water volume and temperature of a crater lake in

Aso volcano, Japan: implications for a sensitive window of a volcanic hydrothermal system. Earth Planets Space 60(6):705–710. https://doi.org/10.1186/bf03353134

Terada A, Hashimoto H, Kagiyama T (2012) A water flow model of the active crater lake at Aso volcano, Japan: fluctuations of magmatic gas and groundwater fluxes from the underlying hydrothermal system. Bull Volcanol 74(3):641–655. https://doi.org/10.1007/s00445-011-0550-4

Thompson G, McNutt S, Tytgat G (2002) Three distinct regimes of volcanic tremor associated with the eruption of Shishaldin Volcano, Alaska 1999. Bull Volcanol 64(8):535–547. https://doi.org/10.1007/s00445-002-0228-z

Ueno H, Hatakeyama S, Aketagawa T, Funasaki J, Hamada N (2002) Improvement of hypocenter determination procedures in the Japan Meteorological Agency. Q J Seismol 65:123–134

Wegler U (2003) Analysis of multiple scattering at Vesuvius volcano, Italy, using data of the TomoVes active seismic experiment. J Volcanol Geotherm Res 128:45–63. https://doi.org/10.1016/S0377-0273(03)00246-4

Wegler U, Lühr BG (2001) scattering behavior at Merapi volcano (Java) revealed from an active seismic experiment. Geophys J Int 145:579–592. https://doi.org/10.1046/j.1365-246x.2001.01390.x

Yamamoto M (2004) Volcanic fluid system inferred from broadband seismic signals. Ph.D. thesis, University of Tokyo, Earthquake Research Institute

Yamamoto M, Kawakatsu H, Kaneshima S, Mori T, Tsutsui T, Sudo Y, Morita Y (1999) Detection of a crack-like conduit beneath the active crater at Aso Volcano. Japan. Geophys Res Lett 26(24):3677–3680. https://doi.org/10.1029/1999GL005395

Yokoo A, Miyabuchi Y (2015) Eruption at the Nakadake 1st crater of Aso volcano started in November 2014. Bull Volcanol Soc Jpn 60(2):275–278. https://doi.org/10.18940/kazan.60.2_275